Journal of Petroleum Science and Engineering 141 (2016) 144–156

Contents lists available at ScienceDirect

Journal of Petroleum Science and Engineering

journal homepage: www.elsevier.com/locate/petrol

Determination of the most significant variables affecting the steady state pressure drop in selected foam flow experiments

Rahul Thorat *, Hans Bruining

Delft University of Technology, Faculty of Civil Engineering and Geosciences, Section of Petroleum Engineering, Netherlands

ARTICLE INFO

Article history:
Received 2 May 2015
Received in revised form
18 September 2015
Accepted 1 December 2015
Available online 19 January 2016

Keywords:
Most significant variables
Interactive effect
Foam experiments
Pressure history
Symbolic regression
Bootstrap method

ABSTRACT

Foam generated with a surfactant solution and nitrogen is used for oil recovery, acid diversion and aquifer remediation. In laboratory experiments, the foam mobility is expressed in terms of the pressure drop across the porous medium and is related to many physical processes. There is lack of data that relate the pressure drop to a combination of three or more variables simultaneously. This paper investigates the steady state pressure drop for a combination of six variables, viz., permeability, surfactant concentration, pH, salinity, surfactant solution velocity and gas velocity. Fourteen pressure drop histories were measured for an Alpha Olefin Sulphonate solution before and after the injection of nitrogen gas across the unconsolidated sandpacks of two median grain sizes and across a Bentheimer consolidated core. Our data set was combined with data sets from the literature leading to 157 data points. Symbolic regression was applied to the entire data set to produce a number of analytical expressions describing the interactive effect of the variables without prior knowledge of an underlying physical process. A simple model with only one fitting parameter was selected to compare with the experimental data. The slope between the observed pressure drop and the predicted pressure drop turns out to be 0.85 ± 0.03. A sensitivity analysis of the chosen model shows that the variables affecting the predicted pressure drop, in order of importance, are permeability, salinity and surfactant solution velocity. The precision of the model parameter was determined by a bootstrap method. The pressure drop from our data set and one specific data set from the literature show significant deviation with respect to the pressure drop obtained from the regression equation. Possible reasons are that the specific data set from the literature uses mixtures of surfactants and that our data set is confined to conditions that lead to low pressure drops. The purpose of the data driven model applied to experimental data is only to improve the models based on physical processes, i.e., mechanistic models. In addition the data driven model can indicate the variable spaces for which more experiments are needed.

1. Introduction

Nitrogen foam (a mixture of nitrogen gas and surfactant with water) can reduce the mobility of a displacing mixture (dispersion) of water and gas, thereby increasing the oil recovery (Bond and Holbrook, 1958; Craig and Lummus, 1965; Holm, 1968; Farajzadeh et al., 2012). Other applications of nitrogen foam are acid diversion (Xu and Rossen, 2003) and aquifer remediation (Wang and Mulligan, 2004). The foam mobility reduction, essential for such applications of foam, is attributed to a reduction in the permeability of the porous medium to the gas (Bernard and Holm, 1964; Friedmann and Jensen, 1986) and/or to an increase of the gas viscosity (Svorstøl et al., 1996). In the laboratory, foam is generated by (1) co-injection of gas and surfactant solution in a porous medium pre-saturated with surfactant (Friedmann et al., 1991; Chou, 1991) or (2) by injection of alternate slugs of gas and surfactant solution through the core (Friedmann and Jensen, 1986; Rossen and Gauglitz, 1990). The surfactant lowers the surface tension of the solution and thereby, with the gas, creates and sustains lamellae in the porous medium. The gas trapped by the lamellae (Hirasaki and Lawson, 1985; Falls et al., 1989) and the immobile fraction of gas (Cohen et al., 1997; Tang and Kovscek, 2006; Nguyen et al., 2007; Balan et al., 2011) result into a pressure drop increase across the porous medium. Foam propagation occurs in two states: an initial unsteady state, characterized by an increase in pressure drop and later, a steady state, where the pressure drop becomes constant. The steady state pressure drop occurs when all transport processes affecting the pressure drop, viz., convection, diffusion, generation and destruction add up to zero (Ashoori et al., 2011). During the steady state, foam propagation through porous media can be described with the two-phase Darcy's law (Holm, 1968). In other words, gas is considered to travel

* Corresponding author.
E-mail address: r.r.thorat@tudelft.nl (R. Thorat).

http://dx.doi.org/10.1016/j.petrol.2015.12.001
0920-4105/

through the porous medium as a separate phase and the flow rate is determined by the relative permeabilities (Buckley and Leverett, 1942). In such a steady state, the gas mobility can be expressed as a ratio of the effective permeability and the apparent viscosity, i.e., k_e/μ_a. Furthermore, the gas mobility is related to the flow rate of foam and the pressure drop observed across the core (Osterloh and Jante, 1992). The gas mobility is affected by a boundary condition where no water exits the core until $S_w = 1 - S_{gr}$ (S_{gr} is irreducible gas saturation and S_w water saturation) is the so-called capillary end effect condition (Barenblatt et al., 1989). Such condition leads to an enhanced saturation at the end of the core (Yortsos and Chang, 1990) and may cause a non-representative value of the pressure drop in the measurement during experimentation (Osoba et al., 1951). Eliminating errors due to the capillary end effect can be achieved by (1) measuring the saturation far enough away from the outflow face (Penn State Method) and (2) using high flow rates to make the error in the measured saturation negligible (Gas flow method) (Osoba et al., 1951).

The observed steady state pressure drop can be further used to calculate the foam resistance factor (Pang, 2010) or mobility reduction factor (Simjoo et al., 2013). The steady state pressure drop is affected by several variables, i.e., permeability of the porous medium, surfactant formulation/concentration, injection rates, presence of oil, gas fraction, temperature, etc. (Friedmann and Jensen, 1986; Friedmann et al., 1991; Isaacs et al., 1988; Huh and Handy, 1989; Hanssen, 1993; Bertin et al., 1999; Simjoo, 2012; Solbakken et al., 2014; Kapetas et al., 2015). Therefore, the steady state pressure drop during foam flow through porous media depends on a complex system of multiple variables. To simplify the complex system of multiple variables, most research studies focus on a base case after which they modify one or two variable(s) at a time, to study their effect on the steady state pressure drop, for example, flow rate and concentration (Fergui et al., 1998) or gas velocity and surfactant solution velocity (Martinez, 1998; Martinez et al., 2001). In addition, such studies use a physical base to construct a model for explaining the steady state, i.e., a mechanistic approach (Kovscek et al., 1997; Rossen et al., 1999). In this respect, Khatib et al. (1988) explained his experiments with a model based on the capillary pressure (pressure difference between gas and surfactant solution phase), which itself depends on the surfactant formulation, the permeability and the gas velocity. However, some other researchers (de Vries and Wit, 1990; Persoff et al., 1991) observed that the steady state pressure drop is a function of the permeability and surfactant velocity, dominated by bubble trapping and mobilization. To explain both contrasting results, Osterloh and Jante (1992) and further Rossen et al. (1995) and Rossen and Wang (1999) proposed two regions in the pressure drop contour plot vs. gas and surfactant solution velocity for a given surfactant formulation and permeability. The region in the pressure drop contour plot, where the pressure drop is nearly independent of the gas velocity, is called the high quality region; the term “quality” is defined as the ratio of gas volume and total, i.e., gas plus surfactant solution volume. The region in the pressure drop contour plot, where the pressure drop is nearly independent of surfactant solution velocity, is called the low quality region. Martinez (1998) and Martinez et al. (2001) introduced the concept of critical foam quality to distinguish between the two regions. In addition, there are other models based on the concepts of local equilibrium (foam texture is an algebraic function of local conditions (Rossen et al., 1999; Ma et al., 2014; Rossen and Boeije, 2015; Boeije and Rossen, 2015) and foam bubble population (Kovscek et al., 1997; Falls et al., 1988; Bertin et al., 1998; Ettinger and Radke, 1992; Kam and Rossen, 2003; Zitha et al., 2006). The difference between local steady state and bubble population models is well described in Ma et al. (2015). In combination with the mechanistic approaches discussed above, Zhao et al. (2012) studied the effect of salinity and surfactant formulation on the steady state pressure drop by orthogonal experiments (Montegomery, 2007) to increase the oil displacement efficiency. Similarly, Wang et al. (2012) studied the quantitative effect of surfactant concentration, foam quality, temperature and oil saturation on the steady state pressure drop by design and analysis of experiment (DAOE) methodology (Montegomery, 2007). The ensuing polynomial expression consists of the product of the individual effects of interacting variables, e.g., foam quality and surfactant concentration, along with a fitting parameter for each combination of the variables to accommodate the interactive effect. Among the variables, the effect of pH on the liquid film for the applications in porous media has been well considered (Nguyen et al., 2002; Farajzadeh et al., 2011), however, not in combination with other variables.

The modeling approaches mentioned above pose practical difficulties for reasons of the required large number of experiments and the large number of fitting parameters. For example, the high and low quality regions for constant permeability and constant surfactant concentration are found by doing experiments for a range of combination of gas and surfactant solution velocities (Ma et al., 2013; Boeije and Rossen, 2013). Such models require physical understanding and are difficult to derive for such a complex system as foam flow. In addition, there is a lack of experimental data that combine orthogonal or even box design (Mason et al., 2003) for variables such as permeability, surfactant concentration, foam quality and salinity affecting the pressure drop. It is difficult to generalize conclusions from the literature as those studies are (deliberately) designed to be unique and are intended for restricted variable spaces. One might ask: (i) can limited experimental data with DAOE methodology represent the whole population of foam experiments from the literature?, (ii) is there a way to use the previous experimental results to generalize the effect of various variables on the steady state pressure drop? and finally, (iii) can we rank the effect of variables on the pressure drop? The path towards resolving these questions could be elucidated with data driven models constructed by applying regression to experimental results. However, conventional regression involves a presumed interrelationship between the variables, which might miss the importance of one variable over another affecting the pressure drop. Therefore, we are motivated to find the hierarchy between the variables with a maximally feasible set of experiments using a non-conventional regression analysis called symbolic regression (Schmidt and Lipson, 2009; Vladislavleva et al., 2010). Symbolic regression, with its ability to search for the model that best describes the data behavior without imposing a priori assumptions, would offer the advantage over conventional multiple regression. Based on a literature survey, we attempt the random variation of six experimental variables, viz., permeability (1860 Darcy, 130 Darcy and 3 Darcy), the concentration of surfactant (0.0375 w/w%, 0.075 w/w% and 0.15 w/w%), gas and surfactant solution velocity (0.27–3.97 m/day), salinity (zero, 0.5 M NaCl) and the pH (6.5, 3.0) as representative conditions in a reservoir. Complimentary to studies conducted in the literature (Simjoo et al., 2013), experiments were conducted with Bentheimer with a low AOS concentration (0.0375 w/w%) and at a low gas fraction ($\approx$ 24%) for two injection rates. Such random variation would circumvent the practical difficulty of conducting an infeasible number of experiments (orthogonal or box design) to rank the variables with respect to their relative importance to affect the pressure drop. Our experiments were designed to add data points that are at conditions less studied in the literature. To overcome the difficulty of statistical inference with only 14 (our) data points, we add 112 data points from Martinez (1998) and Martinez et al. (2001), 21 data points from Osterloh and Jante (1992) and 12 data points from Persoff et al. (1991). The selected data points were similar in some experimental conditions (surfactant-nitrogen co-injection)

and surfactant solutions (AOS), but also had slight variations, viz., single experiment with various steady state pressure drop values corresponding to various gas and surfactant solution velocities: Martinez (1998) and Martinez et al. (2001) and mixing of two surfactants: Osterloh and Jante (1992). The experimental results from the literature were used along with our own results to search for the model form that best describes the data behavior using a minimal number of fitting parameters. We used a freely downloadable software Eureqa® (Nutonian, 2015) with the aforementioned data set to create a host of model expressions. To select a model from the candidate expressions, we used Akaike's information criterion (AIC) (Akaike, 1974), which measures the goodness of fit of the statistical models by incorporating both the likelihood of the model and a penalty for extra parameters.

In addition to criteria for model selection, accurate model verification/validation is also important to assess the merit of the selected model. The sensitivity of the predicted pressure drop to the variable in the model was characterized by the symbolic regression software. Further, we compared the observed pressure drop and the predicted pressure drop by plotting them on *Y*- and *X*-axis respectively. The traditional approach of using the same data, both to construct the model and to estimate its predictive performance, tends to bias the estimate of the model-prediction error. The fitted parameters are connected with the original data set and therefore cannot necessarily be used for different data sets (Olden and Jackson, 2000). The approach of cutting the data in half (one half for modeling and another half for validation) has a drawback of not utilizing precious data points for model building. Therefore, for the purpose of validating the model, a bootstrap method (Efron and Tibshirani, 1993; Press et al., 2007) was used to generate 50 simulated data sets different from the original data set. A given bootstrap sample data set consists of some original data points repeated in the set while some appear only once and some not at all Vittinghoff et al. (2012). The standard deviation obtained from the 50 data sets was used to determine the precision of the fitting parameter of the model.

The paper is structured as follows. For the purpose of describing our data set, we explain the experimental procedure in Section 2 for co-injection of nitrogen and water with dissolved surfactant in different porous media, namely (1) an unconsolidated sandpack of 1860 Darcy, (2) an unconsolidated sandpack of 130 Darcy of 15 cm and (3) a consolidated Bentheimer core of 3 Darcy of 17 cm. The porous media/solutions and the set up are described in Section 2.1 and in Section 2.2 respectively. Section 2.3 describes 14 experiments with the random variation of six experimental variables, viz., permeability, salinity (NaCl), surfactant concentration, pH (hydrogen ion concentration), surfactant solution velocity and gas velocity. In Section 3, the steady state pressure drop measured across the porous medium is reported to show the effect of the used variables on foam flow. In Section 3.1, application of symbolic regression on 157 experimental data points is explained. A procedure is given for an optimal choice of the selected rational expression with fitting parameter A_0. Furthermore, the simplest bootstrap method is used to get 50 simulated data sets. The model from symbolic regression with the fitting parameter A_0 is applied to 50 data sets. A parameter for each simulated data set (A_1^S–A_{50}^S) has been found by variance minimization between predicted and observed pressure drop in Microsoft Excel®. The deviation of those simulated parameters with respect to the predicted parameter is used to estimate the error in the predicted parameter. The experimental results in Section 4.1 are compared for the relationship between the variables and their interactive effect on the pressure drop. One of the most important results is the analysis that shows the missing data, necessary to find the interdependence of the variables affecting the pressure drop. In Section 4.2, the merit and drawback of symbolic regression and the bootstrap method are discussed. We end with some conclusions in Section 5 about the experimental procedure, about the symbolic regression and about the estimate of the observed pressure drop.

2. Experimental section

2.1. Porous media and surfactant solutions

Three types of porous media were used for the foam flow experiments, viz., coarse sand, fine sand and Bentheimer cores. Table 1 shows the grain size, porosity, permeability and length of the porous media. The surface area of 259 grains each for fine and coarse sand was measured under the optical microscope. The particle size was calculated by $\sqrt{4AB/\pi}$, where A is the surface area and B is the roundness. We selected median size of the sample. Prior to its use the sand was treated with a potassium-dichromate-sulfuric acid solution to make it completely water-wet. It was kept in the acid for one day and rinsed with tap water until all the acid was removed according to the procedure mentioned by Furniss et al. (1989). Subsequently the sand was dried and poured, using the procedure of the seven sieves (Wygal, 1963), in an acrylic tube to which we refer as the sandpack. In case of Bentheimer, the core for the experiment was cut from larger samples and was not pretreated prior to its usage. The porosity of the unconsolidated coarse and fine sandpack were assumed (Panda and Lake, 1994), while the porosity of the Bentheimer core was measured by comparing its weight with and without water. The permeability of the sandpack and core were measured by a single phase water permeability test prior to foam flow experiments. Figs. 1(a) and (b) show photographs of the unconsolidated sandpack and the Bentheimer core respectively with the positions for the measurement of the pressure difference. Four pressure measurement points were used, viz., at the outlet, inlet, and two (for a pressure difference meter) in the middle at a distance of 0.06 m apart for the sandpack and 0.09 m apart for the Bentheimer core. The advantage of the short core is that experiments can be finished faster while the disadvantages of the short cores for foam experiments are mainly capillary entry and end effect that affects foam mobility measurements (Reviewer, 2015). We used a 39.1 w/w% Bio–TERGE® AS-40 Sodium C_{14}–C_{16} Alpha-Olefin-Sulfonate (AOS) to prepare 0.3 w/w% AOS solution in both: a 3 w/w% brine (0.5 M $\pm$ 0.01 NaCl) and double distilled water with dissolved HCl (pH = 3.0 $\pm$ 0.3). Both solutions were further diluted to prepare a 0.075 w/w% AOS solution in 0.3 w/w% brine for the unconsolidated coarse sandpack and a 0.0375 w/w% AOS in acidic water for Bentheimer. For the fine sandpack we used an AOS solution in double distilled water (pH = 6.5 $\pm$ 0.2) with varying concentration (0.0375, 0.075, 0.15 w/w%) for various experiments.

2.2. Experimental set up and procedure

Table 2 gives measured property, brand/model, range and accuracy of the instruments used in the set up. Fig. 2 shows the photograph of right side of the set up. The surfactant solution from

Table 1
Porous media used in the experiments.

Porous media	Length (mm)	Median grain size (mm)	Porosity (%)	Permeability (Darcy)
Coarse sand	150	1.00 $\pm$ 0.12	38	1860 $\pm$ 100
Fine sand	150	0.30 $\pm$ 0.08	30	130 $\pm$ 30
Bentheimer	170	–	21 $\pm$ 1	3.0 $\pm$ 0.5

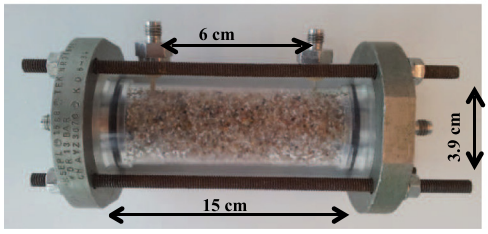

(a) Sandpack with the coarse grains of size ≈ 1 mm. Later experiments were conducted with the fine grains of size ≈ 0.3 mm.

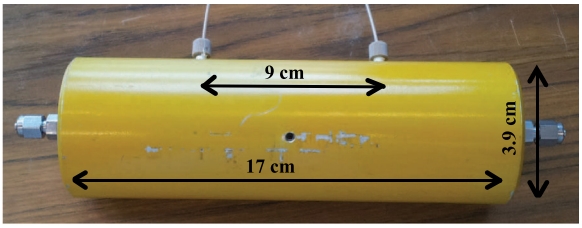

(b) Bentheimer core fitted in the yellow core holder.

Fig. 1. Porous Media (For interpretation of the references to color in this figure caption, the reader is referred to the web version of this paper.)

Table 2
Technical specification of the instruments used in the experiments.

Instrument	Measurement	Unit	Brand/model	Range	Accuracy ±
Reciprocating pump	Surfactant solution mass	ml/h	Pharmacia P-900	0–500	1.5–2
Manometer	Pressure	bar	Endress+Houser	0–65	0.1
Manometer	Pressure difference	bar	Endress+Houser	0–3	0.03
Flow controller	Gas mass	slpm[a]	Sierra instruments[b]	0–1000	10

[a] Standard liter per minute.
[b] Smart Trak® 2 100.

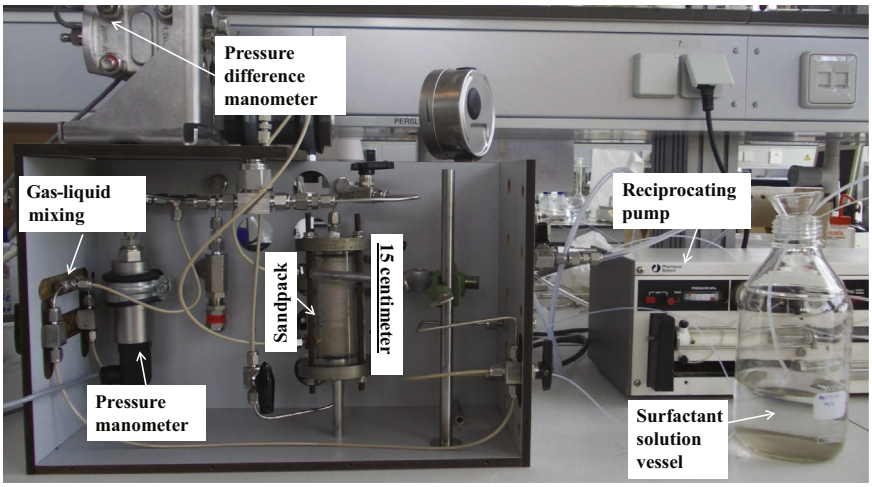

Fig. 2. Photograph of the right side of the set up (injection module). The surfactant solution was pumped from the vessel by the reciprocating pump to mix with the nitrogen gas at the mixing junction. The foam went further through the inlet pressure manometer, foam generator and finally into the porous medium.

a storage vessel was pumped into the porous medium by a pump of the reciprocating type (two cylinders, one for injection and one for refill). The storage vessel was connected to the pump by nylon tubing with an inside diameter of 2 mm and an approximate length of 1 m. Nitrogen gas from the gas supply system at a pressure 7.0 ± 0.1 barA (absolute pressure) was mixed with surfactant solution 30 cm before the injection point of the sample. A flow distributor was used at the bottom and the top between injection tube and sandpack to avoid spurious entrance and production effects. The flow distributor at the bottom of the sandpack contained a steel and nylon filter of mesh size 10/cm and a thickness of 0.12 mm to avoid sand spillage. The direction of the flow in the porous medium was changed for the specific experiments by switching valves at the top and bottom of the porous medium sample. Fig. 3 shows the photograph of left side of the set up. The flow rate of the injected mass was of the range $5.5–175.0 \times 10^{-9}$ kg/s and kept constant during the foam experiment. The foam was collected in the production vessel after it passed through the porous medium. The back pressure valve was regulated by high pressure nitrogen from a cylinder, not shown in the photographs. The manometers (inlet pressure, outlet pressure and pressure difference) were connected to a data acquisition system and a computer to record the pressures versus time. The pressure manometers were calibrated with a pressure calibrator 2095PC (range 1–10 bar and 3–100 bar). We did not measure the temperature in the sandpack experiments. In case of the Bentheimer core experiments, a Platinum/Rhodium alloy thermocouple of type R was used to measure the temperature at the inlet of the core and had a sensitivity of 10.0 μV/°C.

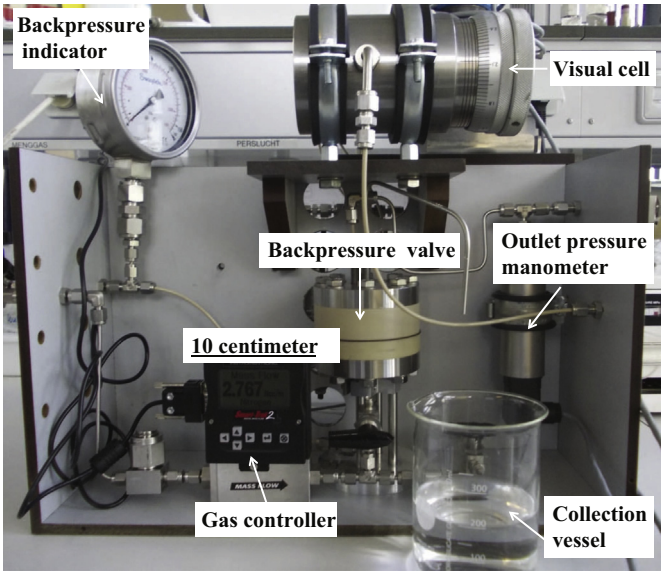

Fig. 3. Photograph of the left side of the set up (production module). After the porous medium, the foam went through the visual cell, the pressure manometer and the back pressure valve. Finally, it was collected in the fluid collection vessel. The gas controller seen here was a part of the injection module to let the nitrogen gas in the mixing zone in the right side of the set up (Fig. 2).

2.3. Foam flow experiments

Fourteen experiments are reported here, i.e., five with coarse sandpack, seven with fine sandpack and two with a Bentheimer sandstone core. All experiments were carried out at room temperature. As the experiments were conducted during day time only, we assume a temperature fluctuation of 3–5 °C. Table 3 shows porous media, test name, time, date, back pressure, surfactant concentration, medium, flow direction, injected surfactant velocity and the pore volume injected (PV) before the start of gas injection for each experiment. PV of the injected surfactant solution was calculated by $(u_l t)/(\phi L)$ where u_l is the surfactant solution velocity (m/s), t is the time (seconds), ϕ is the porosity of the porous media and L is the distance (m) across measurement points. Table 3 further shows the pressure at the inlet manometer (P_{in}), pressure at the outlet manometer (P_{out}) and the pressure difference across the measurement points of the porous medium (ΔP), before the start of the experiments and during the steady flow of single phase surfactant solution. Table 4 focuses on the steady state foam flow after the surfactant solution and gas mixing. The gas velocity at the inlet of the porous medium during steady state (u_g^{ss}) depends on the pressure at the inlet (P_{in}), therefore, was calculated by dividing the injected gas velocity by the pressure ratio at the inlet manometer. The total superficial velocity u_t is the addition of the corrected gas steady state velocity u_g^{ss} and the surfactant solution velocity u_l. Other parameters mentioned in Table 4 are back pressure (BP, barA), the quality of the flow ($\eta_{ss} = u_g^{ss}/u_t^{ss}$) and the foam pressure drop ΔP_f at steady state.

Coarse sandpack: A surfactant solution with a concentration of 0.075 w/w% AOS in 0.5 M brine (NaCl) was used for all experiments in the unconsolidated sandpack of 1860 Darcy. The flow was from the bottom to the top of the sandpack. The first foam experiment "A" started on the 14th February 2011 by flushing a surfactant solution at a rate 1.44 m/d using a back pressure of 7 barA. At $t=300$ s, we opened the back pressure valve, thus releasing the back pressure. At $t=811$ s from the start of the experiment, i.e., 500 s after the release of the back pressure valve, nitrogen gas was injected at a rate 3.17 m/d in the already flowing AOS solution 30 cm upstream of the inlet of

Table 3
Experimental details before the gas injection.

Porous media	Test	Date	Time started	Medium	AOS concentration	Initial conditions before start			Entry solution	Steady state single phase AOS				AOS solution before gas injection PV
						P_{in}	P_{out}	$\Delta P \times 10^4$		u_l	P_{in}	P_{out}	$\Delta P \times 10^4$	PV
		dd/mm/yy	hh:mm		w/w%	barA	barA	Pa/m		m/d	barA	barA	Pa/m	
Coarse	A	14/02/11	16:33	0.5 M Brine	0.075	7.33	7.22	8.00	bottom	1.44	1.67	1.18	3.67	0.6
	B	15/02/11	09:43	0.5 M Brine	0.075	1.53	1.18	15.30	bottom	1.44	4.83	2.26	8.67	2.5
	C	17/02/11	10:53	0.5 M Brine	0.075	1.87	1.73	22.16	bottom	1.09	8.36	7.51	3.55	1.0
	D	19/02/11	14:43	0.5 M Brine	0.075	2.74	1.36	120.00	bottom	2.76				
	E	21/02/11	10:37	0.5 M Brine	0.075	3.09	1.18		bottom	2.76			1597.26	
Fine	F	24/06/11	09:40	pH 6.5[a]	0.075	1.46	1.00	0.10	top	1.09	8.86	1.07	17.7	1.0
	G	09/08/11	13:47	pH 6.5	0.0375	0.99	1.03	0.87	top	1.09	1.26	1.09	9.00	3.8
	H	19/08/11	07:45	pH 6.5	0.0375	0.95	1.04	−2.54	top	1.09	1.19	1.04	1.40	0.4
	I	19/08/11	15:38	pH 6.5	0.0375	1.26	1.10	17.00	top	1.73	1.26	1.10	26.00	8.0
	X	21/08/11	09:37	pH 6.5	0.15	0.06	1.04	0.58	top	1.73	0.07	1.04	0.88	0.5
	J	22/08/11	15:11	pH 6.5	0.15	2.40	1.34	140.00	top	1.73	2.20	1.19	117.58	
	K	23/08/11	15:38	pH 6.5	0.0375	0.97	1.04	1.21	top	1.73	1.01	1.04	4.22	2.0
	L	29/08/11	10:02	pH 6.5	0.15	0.03	1.04	−1.97	top	1.09	2.01	1.05	4.80	3.0
Bentheimer	M	19/04/12	10:44	pH 3.0[b]	0.0375	3.36	3.35	0.01	top	3.25	4.18	4.12	1.36	4.5
	N	26/09/12	13:37	pH 3.0	0.0375	1.21	1.22	−0.13	top	0.81	4.74	4.72	1.14	3.5

P_{in}, pressure at inlet manometer; P_{out}, pressure at outlet manometer; U_l, surfactant solution velocity; *AOS*, Alpha Olefin Sulfonate; ΔP, pressure drop across the measuring points; *PV*, Pore volume of surfactant solution.

[a] pH value fluctuated ± 0.2 in double distilled water.

[b] pH value fluctuated ± 0.3 in double distilled water with HCl.

Table 4
Experimental details during the steady state foam flow after the gas injection.

Porous media	Test	BP	u_g^{st}	P_1^{ss}	u_g^{ss}	u_l	u_t^{ss}	η^{ss}	AOS	$\Delta P_f \times 10^5$
		barA	m/d	Pa	m/d	m/d	m/d	quality	w/w%	Pa/m
Coarse	A	Atm.	3.17	3.56	0.89	1.44	2.33	0.38	0.075	17.0[a]
	B	Atm.	2.17	2.93	0.74	1.44	2.18	0.34	0.075	26.5 ± 0.20
	C	Atm.	1.09	3.30	0.33	1.09	1.41	0.23	0.075	21.0 ± 0.07
	D	Atm.	4.15	3.91	1.06	2.76	3.82	0.28	0.075	26.6 ± 0.03
	E	Atm.	4.15	3.91	1.06	2.76	3.82	0.28	0.075	26.8 ± 0.20
Fine	F	Atm.	5.43	6.96	0.78	1.09	1.87	0.42	0.075	7.5 ± 0.50
	G	Atm.	4.34	2.78	1.56	1.09	2.65	0.59	0.0375	1.5 ± 0.10
	H	Atm.	4.34	1.24	3.50	1.09	4.59	0.76	0.0375	1.6 ± 0.08
	I	Atm.	6.94	1.74	3.97	1.73	5.70	0.70	0.0375	3.7 ± 0.80
	J	Atm.	6.94	2.78	2.49	1.73	4.22	0.59	0.15	15.0 ± 0.10
	K	Atm.	6.94	1.74	3.97	1.73	5.70	0.70	0.0375	3.7 ± 0.20
	L	Atm.	4.15	3.40	1.22	1.09	2.31	0.53	0.15	26.0 ± 0.70
Bentheimer	M	4.1	1.62	1.82	0.89	3.25	4.14	0.22	0.0375	23.7 ± 0.05
	N	4.1	0.41	1.51	0.27	0.81	1.08	0.25	0.0375	42.5 ± 0.10

u_g^{st}, gas velocity at the start; u_l, surfactant solution velocity; *BP*, back pressure; *AOS*, Alpha Olefin Sulphonate; ΔP_f, foam pressure drop.
Steady state: (i) P_1^{ss}, pressure at the inlet; (ii) u_g^{ss}, gas velocity; (iii) u_t^{ss}, total velocity; (iv) η^{ss}, quality.

[a] Steady state pressure drop not recorded due to the limit of the manometer.

the sandpack. We used the same unconsolidated sandpack next day for the next foam experiment "B" with AOS flow rate of 1.44 m/d and a back pressure of 21 barA. At $t=3193$ s, i.e., after flushing 2.5 PV of AOS, we opened the back pressure valve and waited 167 s to open the gas valve. The third foam experiment "C" was started on the 17th February 2011 by flushing the surfactant solution at 1.09 m/d (Thorat and Bruining, 2016). At $t=3309$ s from the start of the experiment, the back pressure valve was opened and at $t=3346$ s, nitrogen gas with an initial gas velocity of 1.62 m/d was injected. We started the next foam experiment "D" on the 19th February 2011 with the same unconsolidated sandpack. The measurement started after an unknown pore volume of 0.075 w/w% AOS was mixed with gas at the total superficial velocity of 3.30 m/d. We repeated experiment "D" on the 21st February 2011, designated as "E".

Fine sandpack: We conducted seven foam experiments with the fine sandpack of 130 Darcy with various AOS solutions (0.0375, 0.075 and 0.15 w/w% in the double distilled water of 6.5 pH) with atmospheric back pressure. The flow direction was from the top to the bottom. The permeability tests were conducted between the foam experiments with tap water as a single phase. The first foam experiment "F" was with 0.075 w/w% AOS. The next experiment "G" was performed on the 9th August 2011 with a low concentration of 0.0375 w/w% AOS. For experiment "H" on the 19th August 2011, the fine sandpack was saturated during the previous evening. After experiment "H", we conducted permeability experiment for three hours with tap water at a varying rate of 0.1–1.0 m/d. Experiment "I" was started on the same day by injecting 0.0375 w/w% AOS at 15:38 at a rate of 1.73 m/d. The foam experiment "X" on the 21st August 2011 was started by injecting 0.15 w/w% AOS solution at 1.73 m/d with an atmospheric back pressure. After four hours (i.e., 70.0 PV injected), the experiment had to be stopped because of lack of solvent. 2.0 PV of surfactant solution were injected on the next day before opening the gas valve for Experiment "J". Experiment "J" was, therefore, considered as a continuation of the previous experiment. Next day on the 23rd August 2011, experiment "I" was repeated under the name "K". After 2158 s, keeping the back pressure atmospheric, nitrogen gas at a flow rate of 6.91 m/d was added to the already flowing 0.0375 w/w% AOS solution. We continued the experiment for four hours, i.e., 40.0 PV. A day before the next foam experiment, we rinsed the sandpack with tap water. We conducted the high concentration 0.15 w/w% AOS experiment "L" on the 29th August 2011 at an injection velocity 1.09 m/d for 5.0 PV of surfactant solution – gas injection.

Bentheimer: Two experiments were carried out with the Bentheimer core of 3 Darcy for low AOS concentration of 0.0375 w/w% in acidic (pH=3.0) water. The back-pressure was kept at 4 barA throughout the experiment. We removed the filter (that generates the foam) and a visual cell (implemented for the observation of foam) to avoid a large pressure gradient at the entrance. Before the experiment started, the Bentheimer core was flushed with CO_2 for five minutes. The CO_2 was followed by 100 ml of double distilled water with HCl (pH 3.0) at a rate 0.61 m/d for five minutes to remove any trapped gas. The foam experiment "M" was started on the 19th April 2012 by flushing the surfactant solution at a velocity of 3.25 m/d. After 97 ml (4.5 PV) of surfactant solution passed into the core, nitrogen gas was injected at a superficial velocity of 1.62 m/d in the already flowing solution. After injection of 700 ml (30 PV) of surfactant solution, the measurements were stopped by closing the gas and liquid flow. The measured temperature fluctuated between 15 and 16 °C. For experiment "N" on the 26th September 2012, we followed the initial steps of the previous experiment. The foam experiment was started by flushing the surfactant solution of 0.0375 w/w% concentration at a velocity of 0.81 m/d in the Bentheimer core. After 78 ml (3.5 PV) of surfactant solution passed into the core, nitrogen gas was mixed at a rate of 0.41 m/d. After the injection of 400 ml (50 PV) of AOS solution the experiment was stopped. The measured temperature fluctuated between 13 °C and 15 °C.

3. Results

The main result is the pressure drop across the measurement points during the steady state foam flow (ΔP_f). From here on, we refer to the pressure drop divided by the distance between the measurement points as the pressure drop, unit Pa/m. The plots contain the observed pressure drop divided by the distance between the measuring points versus the pore volume of surfactant solution and gas injected after opening of the gas valve. The total superficial velocity is calculated by adding surfactant injection velocity and steady state gas velocity, and is given along with the quality (ratio of gas to total velocity) in the brackets. The chronological sequence of the experimental results for each porous medium is given below.

Coarse sandpack: For all experiments with the coarse sandpack of 1860 ± 100 Darcy, we used 0.075 w/w% AOS solution in 0.50 M

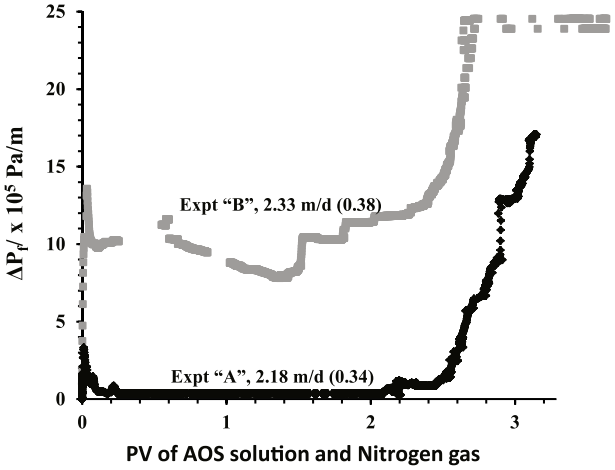

(a) Effect of surfactant adsorption on the pressure drop. The surfactant solutions injected before gas injection were, 0.58 PV for experiment "A" and 2.5 PV for experiment "B".

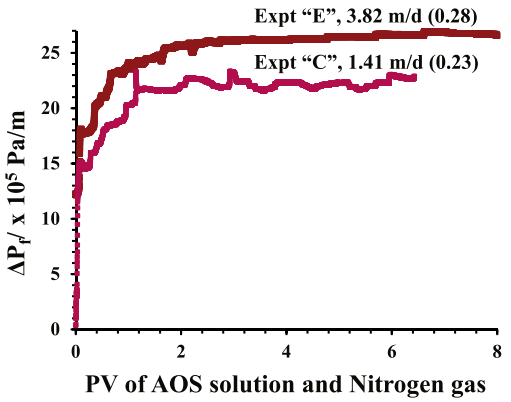

(b) Effect of flow rate on the pressure drop. As the total superficial velocity increased, the pressure drop increased.

Fig. 4. Foam pressure profile for the unconsolidated sandpack of 1860 ± 100 Darcy with 0.075 w/w% AOS solution and nitrogen. The foam quality is mentioned in the brackets here onwards in the figures.

brine. The pressure profiles for the experiment "A" and "B" are shown in Fig. 4(a). For experiment "A", after 2000 s of 2.1 PV of gas and surfactant solution injection, the pressure drop increased rapidly. After 3268 s of 3.1 PV of gas and surfactant solution injection, the pressure drop was 17.0 $\times 10^5$ Pa/m. However, the manometer reached its limit to measure the pressure drop and therefore we could not measure the steady state pressure drop. In case of experiment "B", the pressure drop immediately increased to 10.0×10^5 Pa/m after the injection of gas. During the next 2000 s, i.e, 2.0 PV, the pressure drop did not increase. After t=2560 s of 2.8 PV of gas and surfactant solution injection, the pressure drop fluctuated around $26.5 \pm 0.20 \times 10^5$ Pa/m, which we took as the steady state pressure drop. The steady pressure drop remained around this value during the rest of the experiment for next 2000 s of 2.0 PV injection. Fig. 4(b) shows two experiments "C" and "E" for the total superficial flow velocities 1.41 m/d and 3.82 m/d respectively. In case of experiment "C", we achieved a steady pressure drop of $21.0 \pm 0.07 \times 10^5$ Pa/m after 1.3 PV (Thorat and Bruining, 2016). We continued the experiment for 6.0 PV of surfactant solution–gas mixture. Experiment "E" shows a steady pressure drop of $26.8 \pm 0.2 \times 10^5$ Pa/m after the injection of 5.0 PV for 3000 s. The pressure drop remained steady during the rest of the experiment, i.e., next 6000 s and 15.0 PV.

Fine sandpack: Fig. 5 shows the foam pressure profile for 0.075 w/w% AOS for experiment "F" of 130 Darcy fine sandpack. After an initial fluctuation of 10–15 s due to the opening of the gas valve, a steady pressure drop of 5.0×10^5 Pa/m has been observed. However, after 10.0 PV the pressure drop increased and after 15.0 PV the pressure drop was $7.5 \pm 0.50 \times 10^5$ Pa/m, which we consider as the steady state pressure drop. Fig. 6(a) shows the pressure drop for experiments "H" and "I" using 0.0375 w/w % AOS. A sudden jump in the pressure drop upon nitrogen injection was observed in both experiments. In experiment "H", the pressure drop decreased steadily to a steady value of $1.6 \pm 0.08 \times 10^5$ Pa/m after an initial steep decrease for about 5.0 PV. In experiment "I", which was later repeated as experiment "K", the pressure drop decreased to attain a steady value of $3.7 \pm 0.80 \times 10^5$ Pa/m after

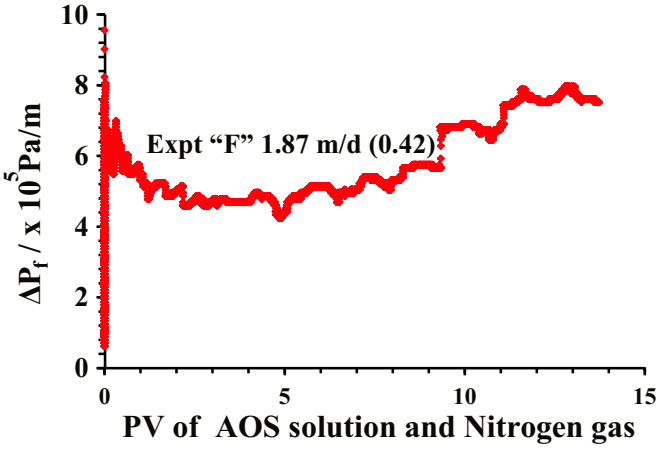

Fig. 5. Foam pressure profile for unconsolidated sandpack (130 Darcy) with 0.075 w/w% AOS solution and nitrogen. We consider the steady state pressure drop to be 7.5×10^5 Pa/m.

about 2 h (20.0 PV). Fig. 6(b) shows the pressure drops for a high AOS concentration (0.15 w/w%) experiments "J" and "L". The steady state values achieved are $15.0 \pm 0.10 \times 10^5$ Pa/m for the high total superficial velocity (4.22 m/d) and $26.0 \pm 0.70 \times 10^5$ Pa/m for the low total superficial velocity (2.31 m/d). For Experiment "J", the pressure drop attained a steady state value of $15.0 \pm 0.10 \times 10^5$ Pa/m after 1.0 PV of surfactant and gas injection. For experiment "L", the pressure drop climbed from a value of 0.48×10^5 Pa/m to a steady pressure drop of $26.0 \pm 0.70 \times 10^5$ Pa/m after 1.5 PV of surfactant solution and gas injection.

Bentheimer: Fig. 7 shows two experiments with the Bentheimer core at a concentration of 0.0375 w/w% AOS solution and a pH of 3.0. The pressure drop for experiment "M" was 2.0×10^4 Pa/m during initial 2.0 PV of AOS-gas injection at a total superficial velocity of 4.14 m/d. The pressure drop achieved a steady value of $23.7 \pm 0.05 \times 10^5$ Pa/m after 10.0 PV were injected. The initial pressure drop for experiment "N" due to gas injection was

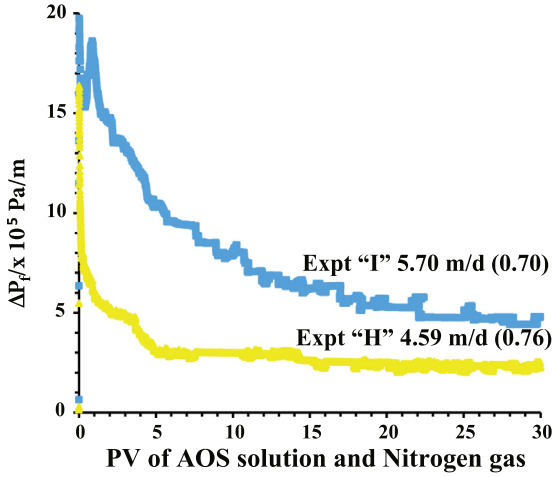

(a) 0.0375 w/w % AOS: As the total superficial velocity increased, the pressure drop increased.

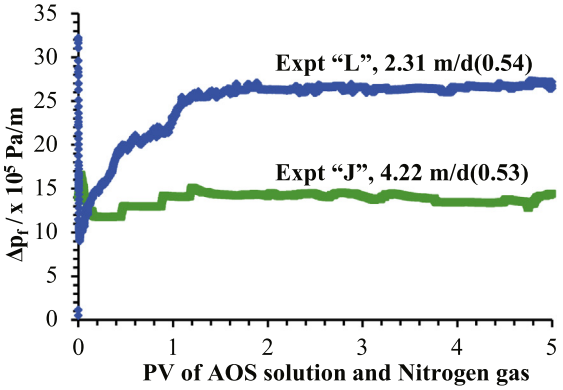

(b) 0.15 w/w % AOS: As the total superficial velocity increased, the pressure drop decreased.

Fig. 6. Foam pressure profile for fine sandpack (130 Darcy). Interactive effect of surfactant concentration and total superficial velocity.

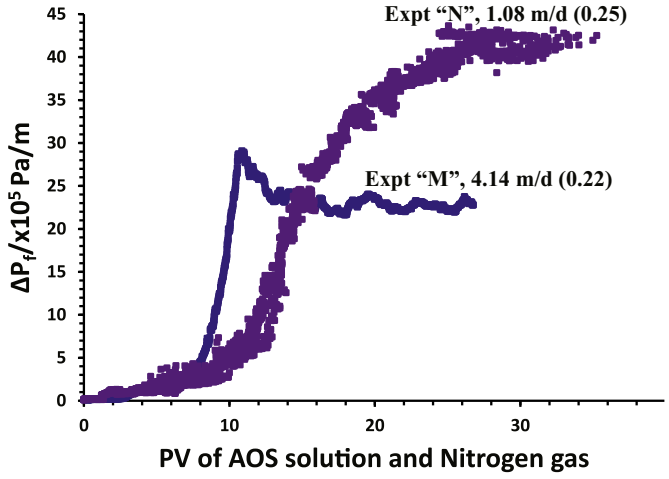

Fig. 7. Foam pressure profile for the Bentheimer core (3 Darcy) with 0.0375 w/w% AOS and nitrogen. The pressure drop increased with the decrease in the total superficial velocity.

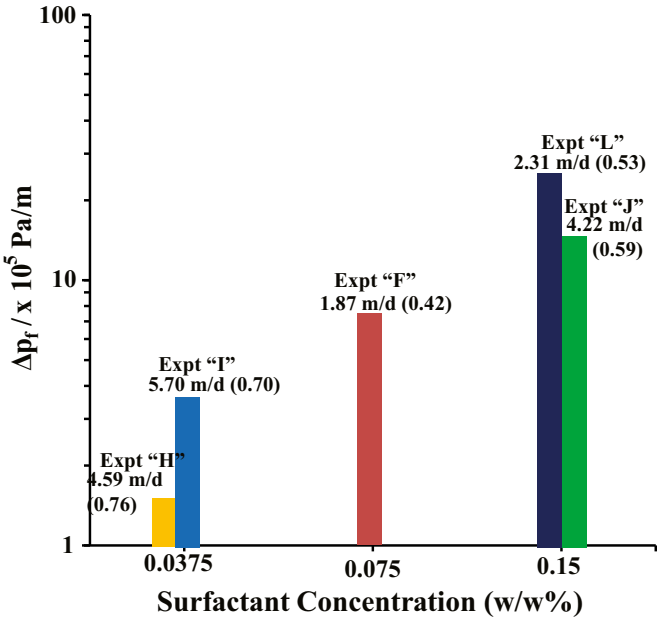

Fig. 8. Summary of experiments with the fine sandpack. Compared to high concentration, the pressure drop in case of low concentration responded opposite to the increase in the total velocity.

9.6×10^4 Pa/m at total superficial velocity 1.08 m/d. After 3.7 PV, the pressure began to increase and around 25.0 PV of gas and AOS injection the pressure drop attained a steady value $42.5 \pm 0.10 \times 10^5$ Pa/m.

3.1. Statistical modeling

Fig. 9 shows the complete procedure of the statistical approach, i.e., data processing, modeling and verification/validation. Based on a literature survey and the experimental results in Table 4 we selected permeability, salinity (NaCl), pH, surfactant concentration, surfactant solution velocity and gas velocity as the independent variables affecting the pressure drop. We coupled our experimental data with the data from Martinez (1998), Martinez et al. (2001), Osterloh and Jante (1992) and Persoff et al. (1991) to get 157 data points. Flow conditions for the data points used from the above literature are given in supplementary information S3, page 7. For our experiment "A", where the pressure crossed the limit of the manometer, we consider maximum observed pressure drop as the steady state pressure drop. The effect of pH is quantified in terms of hydrogen ion concentration, i.e., pH $5.0 = 1 \times 10^{-5}$ mol/l. The cases from the literature are assumed with pH 5.0. We assumed that all data contained same surfactant (AOS, mol/l) and same salinity formulation (NaCl, mol/l). The data are given in the supporting information (Table 1: S2), which can be downloaded from the website. For the modeling part, we used Eureqa® (Nutonian, 2015), a software package based on symbolic regression to determine the relation between the independent variables and the dependent variable, i.e., the observed pressure drop. The software searches the fitting parameters and the form of the equations simultaneously (Schmidt and Lipson, 2009). From these symbolic functions, partial derivatives are derived for the same pairs of

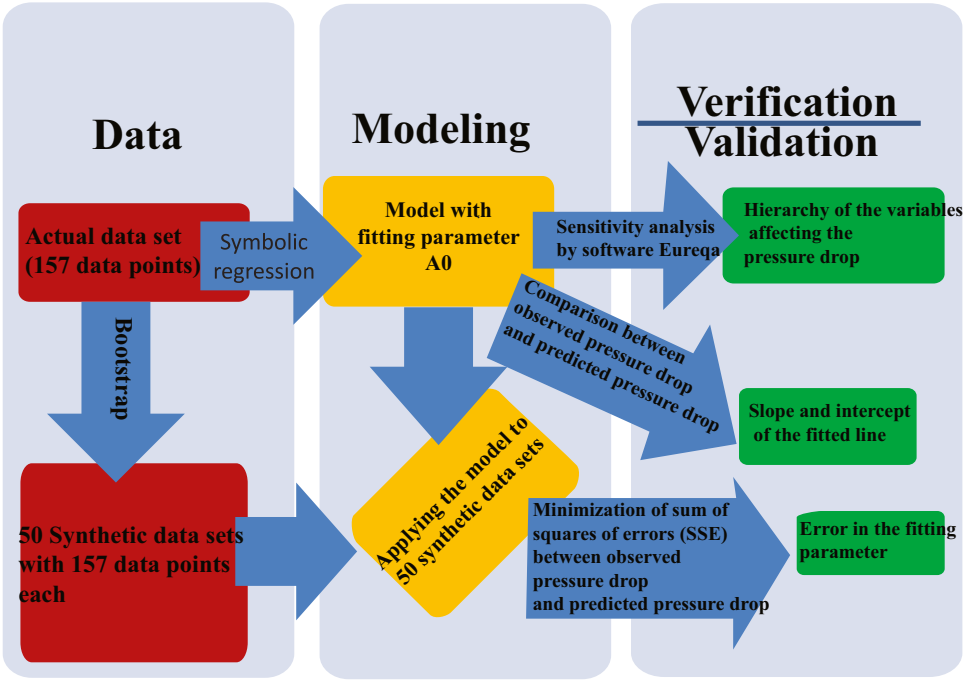

Fig. 9. Statistical modeling of the data.

variables for each candidate function. The steps of deriving numerical and symbolic partial derivatives are repeated to get the best solutions. For more details we suggest the background article (Schmidt and Lipson, 2009) and an article on genetic programming (Veeramachaneni et al., 2012). The software produced a small set of possible analytical expressions given in supporting information (Table 2: S6). We follow the criticism of Dyson (2004) and avoid models with too many fitting parameters. Indeed, a trade off between error and complexity is made to select a model from the expressions, which is of the form:

$$\Delta P = \frac{A_0 NCU_w^{NC}}{\sqrt{k}} \tag{1}$$

where k, NC, and U_w are the permeability (m^2), the salinity, i.e., NaCl (mol/l) and the surfactant solution velocity (m/s). A_0 is the only fitting parameter. ΔP is the predicted (modeled) pressure drop.

The influence of a variable (for example permeability: k) on the independent variable, the predicted pressure drop ΔP was calculated at all input data points. Eureqa uses $|\overline{\partial \Delta P_k}|\sigma(k)/\sigma(\Delta P)$, where $|\overline{\partial \Delta P_k}|$ is the absolute average value of the partial derivative of ΔP with respect to k. $\sigma(k)$ is the standard deviation of k in the input data and $\sigma(\Delta P)$ is the standard deviation of ΔP. If the sensitivity value was 0.5, when the variable k was changed by one standard deviation, the output variable ΔP would change by 0.5 of its standard deviation (Raynolds, 2014). The percentage of data points for which $\partial \Delta P_k > 0$ is denoted by % positive, i.e., the data points for which an increase in the variable k would lead to an increase in the pressure drop, ΔP. The percentage of data points where $\partial \Delta P_k < 0$ is denoted by % negative, i.e., the data points for which an increase in the variable k would lead to a decrease in the pressure drop, ΔP. The magnitude of the positive and negative increase was calculated by $|\overline{\partial \Delta P_k}|\sigma(k)/\sigma(\Delta P)$ for the respective data points. We verified our model further by comparing the observed pressure drop and the predicted pressure drop by plotting them on the Y- and X-axis respectively. We considered a linear model $y(x) = y(x|a, b) = a + bx$, where $y(x)$ is the predicted pressure drop; the fitting parameter "a" is the intercept and the fitting parameter "b" is the slope of the line. As the error in the observed pressure drop was not known, we assumed that all measurements have the same standard deviation. We calculated the intercept, the slope and their respective standard deviations by formulae derived from minimization of the chi-square merit function (Chapter 15, modeling of data from Numerical recipes Press et al., 2007).

For validation, we assumed that the data points were independently and identically distributed. We used a bootstrap procedure involved drawing 157 data points at a time with replacement from the original set by independent random sampling. Because of the replacement, a data set is created in which a random fraction of the original points (typically $1/e = 37\%$) (Press et al., 2007) is replaced by duplicated original points. We generated 50 such synthetic data sets using visual basic in Excel®, each with 157 data points. The data sets are subjected to the same model $\Delta P = A_0 NCU_w^{NC}/K$ as the original data. The fitting parameter for each simulated data set is found by minimizing the sum of squares of difference between predicted pressure drop and observed pressure drop by the Generalized Reduced Gradient (GRG) nonlinear engine in Excel®. The 50 values of the fitted parameters (A_1^s to A_{50}^s) for simulated data set were compared to the original fitted parameter A_0 to obtain the error.

3.2. Statistical results

Table 5 shows the sensitivity analysis for the selected model equation (1). The relative impact of the permeability, salinity and surfactant solution velocity on the pressure drop is 148.8, 14.06 and 0.61 respectively. For all (100%) data points, an increase in the permeability leads to a decrease in the pressure drop with a negative impact of 148.8. For all (100%) data points, an increase in the surfactant solution velocity leads to an increase in the predicted pressure drop, albeit with a small positive impact of 0.61. The effect of salinity for the selected model is ambiguous. Indeed, the salinity (NaCl) for 38% of all data points shows a positive impact with a magnitude of 35.3. But for the remaining 62% of the data points, it decreases with a small negative magnitude of 1.97.

The predicted pressure drop values in Fig. 10 are calculated by

Table 5
Variable sensitivity analysis for the selected model by Eureqa®.

Variable	Sensitivity	Positive (%)	Positive magnitude	Negative (%)	Negative magnitude
Permeability	148.79	0	0	100	148.79
Salinity	14.738	38	35.936	62	1.9755
Water velocity	0.61498	100	0.61498	0	0

Sensitivity, the relative impact that a variable within the model has on the predicted pressure drop; *% Positive*, percent data points, which show an increase in the predicted pressure drop with the increase in the variable; *Positive magnitude*, size of the positive impact; *% Negative*, percent data points, which show a decrease in the predicted pressure drop with the increase in the variable; *Negative magnitude*, size of the negative impact.

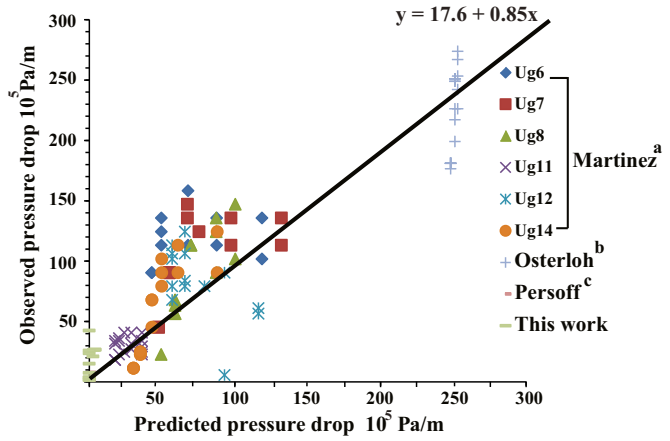

Fig. 10. Precision of the predicted pressure drop from Eq. (1) based on symbolic regression with the experimental pressure drop. The standard deviation in the values of the intercept and slope are 3.20×10^5 Pa/m and 0.03 respectively, calculated by fitting data to a straight line (Press et al., 2007). The mean absolute error in the predicted pressure drop is 21.6×10^5 Pa/m. Data from literature: (a) Martinez (1998), Martinez et al. (2001), (b) Osterloh and Jante (1992) and (c) Persoff et al. (1991).

using Eq. (1) from set of equations (given in supplementary equation S2) generated by symbolic regression using original experimental data from our work and from the literature (given in supplementary section S1). Readers can use the data from supplementary information (given in S1) in freely available software Eureqa to generate set of equations (given in S2). The procedure of generating these equations is briefly discussed in subsection statistical modeling, while the details of the procedure can be found in the work by Schmidt and Lipson (2009). Fig. 10 shows the observed pressure drop from the experiments versus the predicted pressure drop from Eq. (1). The observed pressure drop deviated from the predicted pressure drop by a mean absolute error of $2.16 \pm 0.03 \times 10^6$ Pa/m, which is 10% error for a typical data point of 2.0×10^7 Pa/m. The intercept of the straight line is 17.6×10^5 Pa/m with standard deviation of 3.22×10^5 Pa/m. The slope between the observed pressure drop and the predicted pressure drop data is 0.85 with a standard deviation of 0.03. When the model is applied to 50 data sets with the used bootstrap method, a small error of 3% in the fitting parameter was observed, i.e., $A_0 = 6078 \pm 163$.

The model does not match with the experimental results on the contribution of surfactant concentration (Fig. 8), where the observed pressure drop increases with an increase in the surfactant concentration while other variables (permeability, salinity, etc.) are constant. The model shows considerable discrepancy in the fit for the data points with the lowest observed pressure drop, i.e., our data points. The observed pressure drop in this work is much higher than the predicted pressure drop. Moreover, the model also shows a large discrepancy for the data points with the highest observed pressure drop, i.e., the data points of Osterloh and Jante (1992). Although the model shows some agreement with the data from Martinez (1998) and Martinez et al. (2001), the interactive effect of gas and surfactant solution velocity on the pressure drop as explained in the original article is not observed.

4. Discussion

We split the discussion in two parts, viz., (i) experimental analysis and (ii) statistical analysis. In the experimental analysis we discuss the variables affecting the time to reach the steady state pressure drop and the value of the steady state pressure drop. In the statistical analysis we discuss quantitatively (i) the sensitivity of the pressure drop to the variables from the selected model and (ii) the difference between the predicted pressure drop and observed pressure drop for the data set.

4.1. Experimental analysis

We observed the "S" shaped initial part of the pressure drop curve in all experiments, which represents foam displacing surfactant solution in the AOS saturated core. The gravitational effect due to direction of the flow is found negligible, i.e.,ρ g L$\sim$98 Pa compared to foam pressure, which is of the order 1×10^6 Pa. In case of the same permeability, the steady state pressure drop depended on the initial AOS saturation. For example, the first experiment "A" (Fig. 4(a)) for coarse sandpack, where 0.54 PV surfactant solution was injected before the gas, the effect of foam formation was observed only after 2.0 PV of AOS and gas injection. However, the next experiment "B" (Fig. 4(a)), where 2.5 PV of AOS solution was injected, an immediate increase in the pressure drop after the gas injection was observed. The reason for the delay to reach the steady state pressure drop can be due to a retardation effect caused by the adsorption of surfactant as noted by Chou (1991). When other variables (permeability, AOS conc. and PV of AOS before the gas injection) are the same, the steady state was achieved at different times for different superficial velocities; for example, Bentheimer core with 0.0375 w/w% AOS and $\approx$ 4.0 PV AOS before gas injection. Experiment "M" took 10 PV to attain the steady state pressure drop, while experiment "N" took 20.0 PV, which used one-fourth of the total superficial velocity of experiment "M". From the simulations in our first paper (Thorat and Bruining, 2016), the capillary entry and end effects occur well outside the region where we measure the pressure drop. The simulated saturation during steady state flow for Bentheimer (Expt "M" in the current paper) is almost equal between the measurement points. Similar results can be shown for the sandpack experiments as well. With other variables kept constant (*c.p.*), the steady state pressure drop was observed to increase with increasing surfactant concentration or with increasing total superficial velocity. The low permeability cases, as shown for Bentheimer (Fig. 7) has by far the highest pressure drop, even with the lowest surfactant concentrations and low superficial velocities. In the case of unconsolidated coarse sandpacks (Fig. 4(b) Thorat and Bruining, 2016) and the fine sandpack (Fig. 6(a)), the steady state

pressure drop increased with the increase in the total superficial velocity for constant AOS concentration and constant permeability. In addition, this trend was not affected by a foam quality change. At a high surfactant concentration (0.15 w/w% AOS: Fig. 6(b)) for the case of the fine sandpack and at low concentration for Bentheimer (0.0375 w/w% AOS : Fig. 7), the steady state pressure drop increased with a decrease in the total superficial velocity. The effect can be due to the low gas velocity and due to the high concentration resulting in the creation of numerous thick lamellae. For the same superficial velocities, the increase in AOS concentration (0.0375 w/w% to 0.15 w/w%) resulted in an increase in the pressure drop across the fine sandpack. Therefore we have not found the limit after which the pressure drop does not increase with an increase in the surfactant concentration while maintaining the other variables (permeability, gas velocity and surfactant superficial velocity) constant. We did not have common cases where only pH and the salinity of the water was modified. Therefore we cannot explain their effect on the observed pressure drop. We could not compare our results directly with the results from the literature because the exact combination of the variables we used (permeability, surfactant concentration, gas and surfactant solution velocities, salinity and pH) are not reported there.

4.2. Statistical analysis

The arithmetic expressions given by the symbolic regression allow to express the observed pressure drop in terms of only three variables, viz., permeability, salinity and surfactant solution velocity. Equations with less number of variables, e.g., only permeability, show a worse match as given in supporting information (Table 2 on page S6). If more data were included in the symbolic regression, we might have to include other physical parameters like the gas velocity to explain the observed pressure drop. Extending the data set would also force to consider more parameters (for instance, presence of oil (aromatic or aliphatic) and soil content, etc.) on which the predicted pressure drop depends. However, it is not possible to include each data set which might give the predicted results closer to the experimental results. The generated trend by the symbolic regression for the used data suggests that the gas velocity has no significant effect on the predicted pressure drop for the entire data set as opposed to the pressure drop for a reduced data set. This is because most literature and our data considered in this study are at low foam quality. In case of high foam quality points, at the same permeability and salinity, the observed data points show variation in the pressure drop, while Eq. (1) predicts no variation in the predicted pressure drop. This indicates that more experiments are required in the high quality regime. The large discrepancy for the data points with the highest observed pressure drop, i.e., the data points of Osterloh and Jante (1992) is due to the fact that these data points are obtained for foams that are obtained by mixing two surfactants, viz., AOS (Alpha Olefin Sulphonate) and SDS (Sodium Dodycyl Sulphonate), which is not considered in the equation. Although the equation shows some agreement with the data from Martinez (1998) and Martinez et al. (2001), the interactive effect of gas and surfactant solution velocity on the pressure drop as explained in the original article is not observed. Therefore, a relatively important variable such as the permeability masks the relationships between the variables in the subsets of data. More experiments are needed for conditions for which large deviations between observed and predicted pressure drop occur, i.e., for the extremely low and high experimental pressure drops.

The possible physical mechanism with which salinity affects the foam pressure drop, i.e., stability of foam films, can be explained by the DLVO theory (Overbeek, 1971). The DLVO theory describes the interaction between double layer forces, Van der Waals forces and steric forces. In the absence of surfactant (i.e., no steric forces), an increase in the NaCl concentration would decrease the foam stability as a result of double-layer compression (Wang and Yoon, 2009). However, in the case of the presence of a surfactant, with other variables kept constant (*c.p.*),"We anticipate that (i) at low salt concentration salt mainly affects the charging of a film interface, whereas (ii) at high salt concentration salt mainly affects the screening of the electrostatic repulsion between the two interfaces of the film" (Schelero et al., 2010). Therefore, the effect of salt concentration can only be observed in limited parameter spaces. In addition Eq. (1) needs to be interpreted in a statistical sense, where, for the available data points, the effect of salinity on the predicted pressure drop cannot be viewed in an isolated sense. The only clear trend observed from the equation is that higher pressure drop is obtained for lower permeable media. If we consider Darcy's formula to explain the physical mechanism, higher permeability leads to the lower pressure drop and an increase in water velocity would increase the pressure drop. Eq. (1) is therefore a data driven equation and not based on physical mechanism, as explicitly stated.

5. Conclusions

- We measured fourteen pressure drop histories before and after injection of an Alpha Olefin Sulphonate solution (AOS) with nitrogen gas (N_2) across measurement points in various porous media. All experiments observed an increase in pressure drop when nitrogen was added in the flowing surfactant solution. The initial conditions of the core (gas content, adsorption) influenced the foam generation in the core. It is possible to obtain a steady state pressure drop from the pressure drop histories.
- We measured the steady state pressure drop for unconsolidated sand packs (1860 and 130 Darcy) and a Bentheimer sand stone core (3 Darcy) for various surfactant concentrations (0.0375, 0.075 and 0.15 w/w%), for various gas and surfactant solution velocities (0.27–3.97 m/day), for two salinities (0, 0.5 M NaCl) and for two pHs (6.5, 3.0). The above six variables were varied simultaneously to obtain their interactive effects on the steady state pressure drop. We refer to the pressure drop divided by the distance between the measurement points as the pressure drop (Pa/m). The pressure drop increased with an increase in the total superficial velocity and the AOS concentration while keeping other variables constant (ceteris paribus *c.p.*). For the concentration range studied by us, a limiting surfactant concentration that gives a maximum pressure drop was not observed.
- Symbolic regression can be applied to our data along with 143 data points from the literature to produce a number of analytical expressions without prior knowledge of an underlying physical process. A simple model with a single fitting parameter can be used to describe the pressure drop with three out of the six variables, viz., the permeability, the salinity and the surfactant solution velocity. The model can be verified by a sensitivity analysis, which shows that for the chosen model the variables in order of importance are the permeability, the salinity and the surfactant solution velocity. The model can be validated by estimating the error in the model parameter ($A_0 = 6078 \pm 163$) by the applied bootstrap method. The data driven model can be of help to find the underlying physics of the foam flow through porous media. The purpose of the derived data driven model is not to replace the models based on physical processes, i.e., mechanistic models.
- The observed pressure drop was of the order of 2.00×10^7 Pa/m and deviated from the predicted pressure drop by a mean

absolute error of 2.16×10^6 Pa/m. The intercept and the slope between the observed pressure drop and the predicted pressure drop data are $17.6 \pm 3.22 \times 10^5$ Pa/m and 0.85 ± 0.03 respectively. Our data set and the data set of Osterloh and Jante (1992) show significant deviation from the chosen symbolic regression model, which shows that the model has limitations. Possible reasons are that Osterloh and Jante (1992) use mixtures of surfactants and that our data set is confined to conditions that lead to low pressure drops.

- The model from symbolic regression is able to elucidate the general behavior and hierarchy of the variables affecting the steady state pressure drop. The model gives the variable spaces for which more experiments are needed. Considering an entire data set shows that the trends obtained from a subset of the data are not necessarily valid for the complete data set.

Acknowledgment

We thank Erasmus Mundus-India scholarship program for the scholarship and Shell for financial support. We acknowledge numerous useful suggestions of Prof. Dr. W.R. Rossen. We thank Dr. R. Farajzadeh for initiating the project and Dr. A.A. Eftekhari for information on the software Eureqa®.

Appendix A. Supplementary data

Supplementary data associated with this article can be found in the online version at http://dx.doi.org/10.1016/j.petrol.2015.12.001.

References

Akaike, H., 1974. A new look at the statistical model identification. IEEE Trans. Autom. Control 19 (6), 716–723. http://dx.doi.org/10.1109/TAC.1974.1100705.
Ashoori, E., Marchesin, D., Rossen, W., 2011. Roles of transient and local equilibrium foam behavior in porous media: traveling wave. Colloids Surf. A: Physicochem. Eng. Aspects 377 (13), 228–242. http://dx.doi.org/10.1016/j.colsurfa.2010.12.042.
Balan, H., Balhoff, M.T., Nguyen, Q.P., Rossen, W., 2011. Network modeling of gas trapping and mobility in foam enhanced oil recovery. Energy Fuels 25 (9), 3974–3987. http://dx.doi.org/10.1021/ef2006707.
Barenblatt, V., Entov, G.I., Ryzhik, V., 1989. Theory of Fluid Flows through Natural Rocks. Kluwer, Dordrecht.
Bernard, G.G., Holm, L.W., 1964. Effect of foam on permeability of porous media to gas. SPE J. 4, 267–274. http://dx.doi.org/10.2118/983-PA.
Bertin, H., Quintard, M., Castanier, L., 1998. Development of a bubble-population correlation for foam-flow modeling in porous media. SPE J. 3 (4), 356–362. http://dx.doi.org/10.2118/52596-PA.
Bertin, H.J., Apaydin, O.G., Castanier, L.M., Kovscek, A.R., 1999. Foam flow in heterogeneous porous media: effect of cross flow. SPE J. 4 (2), 75–82. http://dx.doi.org/10.2118/39678-MS.
Boeije, C., Rossen, W., 2013. Fitting foam simulation model parameters to data. In: IOR 2013: 17th European Symposium on Improved Oil Recovery, St. Petersburg, Russia, 16–18 April, EAGE, 1–16, http://dx.doi.org/10.3997/2214-4609.20142604.
Boeije, C., Rossen, W., 2015. Fitting foam-simulation-model parameters to data: I. Coinjection of gas and liquid. SPE Reserv. Eval. Eng. 18, 264–272. http://dx.doi.org/10.2118/174544-PA.
Bond, D., Holbrook, O., 1958. Gas drive oil recovery process. US Patent 2,866,507.
Buckley, S.E., Leverett, M.C., 1942. Mechanism of fluid displacement in sands. Trans. AIME 146 (01), 107–116.
Chou, S., 1991. Conditions for generating foam in porous media. In: SPE Annual Technical Conference and Exhibition, 6–9 October, Dallas, Texas, Society of Petroleum Engineers, pp. 353–364, http://dx.doi.org/10.2118/22628-MS.
Cohen, D., Patzek, T., Radke, C., 1997. Onset of mobilization and the fraction of trapped foam in porous media. Transp. Porous Media 28 (3), 253–284. http://dx.doi.org/10.1023/A:1006552320036, ISSN 0169-3913.
Craig Jr., F., Lummus, J., 1965. Oil recovery by foam drive. US Patent 3,185,634.
de Vries, A.S., Wit, K., 1990. Rheology of gas/water foam in the quality range relevant to steam foam. SPE Reserv. Eng. 5 (2), 185–192. http://dx.doi.org/10.2118/18075-PA.
Dyson, F., 2004. A meeting with Enrico Fermi. Nature 427 (6972), 297. http://dx.doi.org/10.1038/427297a.
Efron, B., Tibshirani, R., 1993. An Introduction to the Bootstrap Monographs on Statistics and Applied Probability vol. 57. Chapman Hall CRC, Dordrecht, Netherlands, ISBN 0412042312.
Ettinger, R.A., Radke, C.J., 1992. Influence of texture on steady foam flow in Berea sandstone. SPE Reserv. Eng. 7 (1), 83–90. http://dx.doi.org/10.2118/19688-PA.
Falls, A., Hirasaki, G., Patzek, T., Gauglitz, D., Miller, D., Ratulowski, T., 1988. Development of a mechanistic foam simulator: the population balance and generation by snap-off. SPE Reserv. Eng. 3 (3), 884–892. http://dx.doi.org/10.2118/14961-PA.
Falls, A., Musters, J., Ratulowski, J., 1989. The apparent viscosity of foams in homogeneous bead packs. SPE Reserv. Eng. 4 (2), 155–164. http://dx.doi.org/10.2118/16048-PA.
Farajzadeh, R., Muruganathan, R.M., Rossen, W.R., Krastev, R., 2011. Effect of gas type on foam film permeability and its implications for foam flow in porous media. Adv. Colloid Interf. Sci. 168 (12), 71–78. http://dx.doi.org/10.1016/j.cis.2011.03.005, ISSN 0001-8686.
Farajzadeh, R., Andrianov, A., Krastev, R., Hirasaki, G.J., Rossen, W.R., 2012. Foam–oil interaction in porous media: implications for foam assisted enhanced oil recovery. Adv. Colloid Interf. Sci. 183–184, 1–13. http://dx.doi.org/10.1016/j.cis.2012.07.002.
Fergui, O., Bertin, H., Quintard, M., 1998. Transient aqueous foam flow in porous media: experiments and modeling. J. Pet. Sci. Eng. 20, 9–29. http://dx.doi.org/10.1016/S0920-4105(98)00036-9, ISSN 0920-4105.
Friedmann, F., Jensen, A., 1986. Some parameters influencing the formation and propagation of foams in porous media. In: SPE California Regional Meeting, 2–4 April, Oakland, California, Society of Petroleum Engineers, pp. 441–454, http://dx.doi.org/10.2118/15087-MS.
Friedmann, F., Chen, W., Gauglitz, P., 1991. Experimental and simulation study of high-temperature foam displacement in porous media. SPE Reserv. Eng. 6 (1), 37–45. http://dx.doi.org/10.2118/17357-PA.
Furniss, B., Hannaford, A., Smith, P., Tatchell, A., 1989. Vogel's Textbook of Practical Organic Chemistry, 5th ed. Longman Group UK Limited, UK.
Hanssen, J.E., 1993. Foam as a gas-blocking agent in petroleum reservoirs I: empirical observations and parametric study. J. Pet. Sci. Eng. 10 (2), 117–133. http://dx.doi.org/10.1016/0920-4105(93)90036-E.
Hirasaki, G., Lawson, J., 1985. Mechanisms of foam flow in porous media: apparent viscosity in smooth capillaries. SPE J. 25 (2), 176–190. http://dx.doi.org/10.2118/12129-PA.
Holm, L., 1968. The mechanism of gas and liquid flow through porous media in the presence of foam. SPE J. 8 (4), 359–369. http://dx.doi.org/10.2118/1848-PA.
Huh, D., Handy, L., 1989. Comparison of steady and unsteady-state flow of gas and foaming solution in porous media. SPE Reserv. Eng. 4 (1), 77–84. http://dx.doi.org/10.2118/15078-PA.
Isaacs, E.E., McCarthy, F.C., Maunder, J.D., 1988. Investigation of foam stability in porous media at elevated temperatures. SPE Reserv. Eng. 3, 565–572. http://dx.doi.org/10.2118/15647-PA.
Kam, S.I., Rossen, W.R., 2003. A model for foam generation in homogeneous media. SPE J. 8 (4), 417–425. http://dx.doi.org/10.2118/87334-PA.
Kapetas, L., Vincent Bonnieu, S., Danelis, S., Farajzadeh, R., Eftekhari, A., Mohd Shafian, S.R., Kamarul Bahrim, R.Z., Rossen, W.R., 2015. Effect of temperature on foam flow in porous media. In: SPE Middle East Oil & Gas Show and Conference, 8–11 March, Manama, Bahrain, Society of Petroleum Engineers, pp. 1–16, http://dx.doi.org/10.2118/172781-MS.
Khatib, Z., Hirasaki, G., Falls, A., 1988. Effects of capillary pressure on coalescence and phase mobilities in foams flowing through porous media. SPE Reserv. Eng. 3 (3), 919–926. http://dx.doi.org/10.2118/15442-PA.
Kovscek, A.R., Patzek, T.W., Radke, C.J., 1997. Mechanistic foam flow simulation in heterogeneous and multidimensional porous media. SPE J. 2 (4), 511–526. http://dx.doi.org/10.2118/39102-PA.
Ma, K., Lopez-Salinas, J.L., Puerto, M.C., Miller, C.A., Biswal, S.L., Hirasaki, G.J., 2013. Estimation of parameters for the simulation of foam flow through porous media. Part 1: the dry-out effect. Energy Fuels 27 (5), 2363–2375. http://dx.doi.org/10.1021/ef302036s.
Ma, K., Lopez-Salinas, J.L., Miller, C.A., Biswal, S.L., Hirasaki, G.J., 2014. Non-uniqueness, numerical artifacts, and parameter sensitivity in simulating steady-state and transient foam flow through porous media. Transp. Porous Media 102 (3), 325–348. http://dx.doi.org/10.1007/s11242-014-0276-9.
Ma, K., Ren, G., Mateen, K., Morrel, D., Cordelier, P., Hirasaki, G.J., 2015. Modeling techniques for foam flow in porous media. SPE J. 20 (3), 453–470. http://dx.doi.org/10.2118/169104-PA.
Martinez, J., 1998. Foam-flow Behaviour in Porous Media: Effects of Flow Regime and Porous-Medium Heterogeneity (Ph.D. thesis). University of Texas at Austin.
Martinez, J., Rivas, H.J., Rossen, W.R., 2001. Unified model for steady-state foam behavior at high and low foam qualities. SPE J. 6 (3), 325–333. http://dx.doi.org/10.2118/74141-PA.
Mason, R., Gunst, R., Hess, J., 2003. Statistical Design and Analysis of Experiments, 2nd ed. John Wiley & Sons, Inc., Hoboken, New Jersey.
Montegomery, D., 2007. Design and Analysis of Experiments, 7th ed. John Wiley & Sons, Inc., Hoboken, New Jersey.
Nguyen, Q., Zitha, P., Currie, P.K., 2002. Effect of foam films on gas diffusion. J. Colloid Interf. Sci. 248 (2), 467–476. http://dx.doi.org/10.1006/jcis.2001.8155.
Nguyen, Q., Currie, P.K., Buijse, M., Zitha, P.L.J., 2007. Mapping of foam mobility in porous media. J. Pet. Sci. Eng. 58 (1), 119–132. http://dx.doi.org/10.1016/j.petrol.2006.12.007.
Nutonian, 2015. Eureqa® Desktop ⟨www.nutonian.com/products/eureqa/⟩.
Olden, J.D., Jackson, D.A., 2000. Torturing data for the sake of generality: how valid

are our regression models?. Ecoscience 7 (4), 501–510, URL: ⟨http://www.jstor.org/stable/42901269⟩.
Osoba, J.S., Richardson, J.G., Kerver, J.K., Hafford, J.A., Blair, P.M., 1951. Laboratory measurements of relative permeability. J. Pet. Technol. 3. http://dx.doi.org/10.2118/951047-G.
Osterloh, W., Jante Jr., M., 1992. Effects of gas and liquid velocity on steady-state foam flow at high temperature. In: SPE/DOE Enhanced Oil Recovery Symposium, 22–24 April, Tulsa, Oklahoma, Society of Petroleum Engineers, pp. 237–248, http://dx.doi.org/10.2118/24179-MS.
Overbeek, J., 1971. Colloid and Surface Chemistry. Lyophobic Colloids, vol. 2. Massacheusetts Institute of Technology, Cambridge, MA.
Panda, M.N., Lake, L.W., 1994. Estimation of single-phase permeability from parameters of particle-size distribution. AAPG Bull. 78 (7), 1028–1039.
Pang, Z.-X., 2010. The blocking ability and flowing characteristics of steady foams in porous media. Transp. Porous Media 85 (1), 299–316. http://dx.doi.org/10.1007/s11242-010-9563-2, ISSN 0169-3913.
Persoff, P., Radke, C., Pruess, K., Benson, S., Witherspoon, P., 1991. A laboratory investigation of foam flow in sandstone at elevated pressure. SPE Reserv. Eng. 6 (3), 365–372. http://dx.doi.org/10.2118/18781-PA.
Press, H., Teukolsky, S.A., Vetterling, W., Flannery, B., 2007. Numerical Recipes, 3rd ed. Cambridge University Press, New York.
Raynolds, A., 2014. Sensitivity Interpretation ⟨http://formulize.nutonian.com/forum⟩.
Reviewer, 2015. Review “Determination of the most significant variables affecting the steady state pressure drop in selected foam flow experiments”. Manuscript number PETROL6802.
Rossen, W.R., Boeije, C.S., 2015. Fitting foam-simulation-model parameters to data: II. Surfactant-alternating-gas foam applications. SPE Reserv. Eval. Eng. 18 (2), 273–283. http://dx.doi.org/10.2118/165282-PA.
Rossen, W.R., Gauglitz, P.A., 1990. Percolation theory of creation and mobilization of foams in porous media. AIChE J. 36 (8), 1176–1188. http://dx.doi.org/10.1002/aic.690360807.
Rossen, W.R., Wang, M.W., 1999. Modeling foams for acid diversion. SPE J. 4, 92–100. http://dx.doi.org/10.2118/56396-PA.
Rossen, W.R., Zhou, Z.H., Mamun, C.K., 1995. Modeling foam mobility in porous media. SPE Adv. Technol. Ser. 3, 146–153. http://dx.doi.org/10.2118/22627-PA.
Rossen, W., Zeilinger, S., Shi, J.-X., Lim, M., 1999. Simplified mechanistic simulation of foam processes in porous media. SPE J. 4 (3), 279–287. http://dx.doi.org/10.2118/57678-PA.
Schelero, N., Hedicke, G., Linse, P., Klitzing, R.v., 2010. Effects of counterions and coions on foam films stabilized by anionic dodecyl sulfate. J. Phys. Chem. B 114 (47), 15523–15529. http://dx.doi.org/10.1021/jp1070488.
Schmidt, M., Lipson, H., 2009. Distilling free-form natural laws from experimental data. Science 324 (5923), 81–85. http://dx.doi.org/10.1126/science.1165893.
Simjoo, M., 2012. Immiscible Foam for Enhanced Oil Recovery (Ph.D. thesis). Delft University of Technology.
Simjoo, M., Dong, Y., Andrianov, A., Talanana, M., Zitha, P.L.J., 2013. Novel insight into foam mobility control. SPE J. 18 (3), 416–427. http://dx.doi.org/10.2118/163092-PA.
Solbakken, J.S., Skauge, A., Aarra, M.G., 2014. Foam performance in low permeability laminated sandstones. Energy Fuels 28 (2), 803–815. http://dx.doi.org/10.1021/ef402020x.
Svorstøl, I., Vassenden, F., Mannhardt, K., 1996. Laboratory studies for design of a foam pilot in the Snorre field. In: SPE/DOE Improved Oil Recovery Symposium, 21–24 April, Tulsa, Oklahoma, Society of Petroleum Engineers, pp. 563–573, http://dx.doi.org/10.2118/35400-MS.
Tang, G.Q., Kovscek, A.R., 2006. Trapped gas fraction during steady-state foam flow. Transp. Porous Media 65 (2), 287–307. http://dx.doi.org/10.1007/s11242-005-6093-4.
Thorat, R., Bruining, H., 2016. Foam flow experiments. I. Estimation of the bubble generation function. Transp. Porous Media, accepted for publication.
Veeramachaneni, K., Vladislavleva, E., O'Reilly, U.M., 2012. Knowledge mining sensory evaluation data: genetic programming, statistical techniques, and swarm optimization. Gen. Programm. Evol. Mach. 13 (1), 103–133. http://dx.doi.org/10.1007/s10710-011-9153-2.
Vittinghoff, E., Glidden, D., Shiboski, S., McCulloch, C., 2012. Basic statistical methods. In: Regression Methods in Biostatistics, Statistics for Biology and Health. Springer, US, pp. 27–67.
Vladislavleva, K., Veeramachaneni, K. O'Reilly, U.M., Burland, M., Parcon, J., 2010. Learning a lot from only a little: genetic programming for panel segmentation on sparse sensory evaluation data. In: Genetic Programming, Lecture Notes in Computer Science, vol. 6021. Springer, Berlin, Heidelberg, ISBN 978-3-642-12147-0, pp. 244–255.
Wang, S., Mulligan, C.N., 2004. An evaluation of surfactant foam technology in remediation of contaminated soil. Chemosphere 57 (9), 1079–1089. http://dx.doi.org/10.1016/j.chemosphere.2004.08.019.
Wang, L., Yoon, R.-H., 2009. Effect of pH and NaCl concentration on the stability of surfactant-free foam films. Langmuir 25 (1), 294–297. http://dx.doi.org/10.1021/la802664k.
Wang, J., Liu, H., Ning, Z., Zhang, H., 2012. Experimental research and quantitative characterization of nitrogen foam blocking characteristics. Energy Fuels 26 (8), 5152–5163. http://dx.doi.org/10.1021/ef300939j.
Wygal, R., 1963. Construction of models that simulate oil reservoirs. SPE J. 3 (4), 281–286. http://dx.doi.org/10.2118/534-PA.
Xu, Q., Rossen, W., 2003. Effective viscosity of foam in periodically constricted tubes. Colloids Surf. A: Physicochem. Eng. Aspects 216 (13), 175–194. http://dx.doi.org/10.1016/S0927-7757(02)00547-2, ISSN 0927-7757.
Yortsos, Y., Chang, J., 1990. Capillary effects in steady-state flow in heterogeneous cores. Transp. Porous Media 5 (4), 399–420. http://dx.doi.org/10.1007/BF01141993, cited by 38.
Zhao, L., Li, A., Chen, K., Tang, J., Fu, S., 2012. Development and evaluation of foaming agents for high salinity tolerance. J. Pet. Sci. Eng. 81, 18–23. http://dx.doi.org/10.1016/j.petrol.2011.11.006.
Zitha, P.L.J., Du, D.X., Uijttenhout, M., Nguyen, Q.P., 2006. Numerical analysis of a new stochastic bubble population foam model. In: SPE/DOE Symposium on Improved Oil Recovery, 22–26 April, Tulsa, USA, Society of Petroleum Engineers, pp. 1–14, http://dx.doi.org/10.2118/99747-MS.